The Role of Porosity in Filtration: Part V.

Porosity Variation in Filter Cakes

F. M. TILLER and HARRISON COOPER

University of Houston, Houston, Texas

Expressions are derived in which local porosity in a filter cake is determined as a function of the distance through the cake. Under conditions where the superficial flow rate through the cake is constant and the medium pressure can be neglected, local porosity and the hydraulic pressure are functions of the fractional cake distance.

Equations are derived that give the average porosity of a cake as a function of applied filtration pressure.

In filter cakes the variation of porosity with distance from the cake surface is important from both theoretical and industrial viewpoints. In the development of filtration theory porosity plays a fundamental role in its relation to flow rates, pressure, and other parameters involved in the differential equations of flow through compressible, porous media. Porosity variation determines the average porosity and liquid content of the filter cake in commercial operation. Since a dry cake is frequently desired, it is important for design purposes to know how the average porosity varies with total pressure. It will be shown that increasing pressure has widely different effects on liquid content. With some materials the average porosity is hardly affected by increasing pressure; with others substantial decreases are involved.

Few investigations of porosity variation have been reported in the literature. Hutto (*4*) developed a unique banding technique in which a colored material was introduced at equal mass intervals and incremental volumes were measured visually. An extensive experimental analysis of porosity variation was made by Shirato and Okamura (*8*), who carefully correlated theory with experiment on the basis of Equations (7) and (9) of this paper. These authors gave plots of porosity ϵ vs. fractional distance x/L through solids as well as of the average porosity ϵ_{avg} and the ratio m of mass of wet to mass of dry cake as functions of total pressure. They showed that ϵ_{avg} varied approximately as a power function of the applied pressure p.

Rietema (*6*) reported porosity distributions in which the porosity reached a minimum in the interior of the cake and then rose before decreasing again. Doubt exists as to the validity of Rietema's results, as they are not in accord with current theory, which leads to a continuously decreasing porosity. He measured the porosity indirectly by attempting to relate electrical resistance of a cake of polyvinyl chloride to porosity.

Hutto (*4*) compared the porosity data of Grace (*2*) and Young (*12*) with his own experimental determinations. Grace's data for calcium carbonate indicated a slow rate of decrease of porosity with distance at the surface of the cake, compared with a more rapid rate of change at the septum. For the substances gyrolite, perlite, diatomite, and wood pulp, however, Hutto found that the porosity decreased most rapidly at the surface, in contrast with Grace's results. As the trends of theoretically calculated values for kaolin (*9*) agreed with his experimental values, Hutto reasoned that Grace's experimental data were in error. It will be demonstrated in this paper that curves of the type shown by both Grace and Hutto can exist along with other possibilities.

EXPERIMENTAL PROCEDURE

In order to calculate the porosity as a function of the distance from the cake surface it is necessary to know the porosity ϵ and the point or local specific filtration resistance α_x as functions of the compressive pressure p_s. These data may be obtained simultaneously with the use of a compression-permeability cell (*2*). It is also possible to use other methods for getting the porosity and specific resistance. The porosity vs. compressive pressure data may be determined in a simple consolidometer (*8, 9*) in which the wet solid is subjected to different loads. The point specific resistance may be found mathematically (*9*) from average values determined directly from constant pressure, constant rate, or variable-pressure–variable-rate filtration.

Grace (*3*) asserted that the variable-pressure–variable-rate procedure was severely limited because of the difficulty of obtaining small centrifugal pumps with high head characteristics. In addition he pointed out that unfavorable shearing action in such pumps may lead to changes in the nature of the particles and to erroneous values for filtration resistance. These difficulties as envisioned by Grace can be overcome by simple piping arrangements employing high head, low capacity, positive displacement pumps. A constant-rate pump combined with a suitable bypass placed between the pump and the filter may be successfully used to produce variable-rate conditions. As the pressure builds in the filter, the rate of flow through the bypass increases and the rate of filtration decreases. By proper setting of the valve in the bypass the maximum pressure can be restricted to any desired value. Small positive-displacement pumps are readily available.

Calculation of Porosity

Formulas for porosity calculations depend upon the basic equations for flow through compressible porous media and the relation between local porosity and applied compressive pressure. Expressions involving numerical integration followed by approximate equations utilizing empirical relations will be developed here.

The basic equation for flow through compressible porous media is given by (*3, 11*)

$$-g_c \frac{dp_x}{dw_x} = g_c \frac{dp_s}{dw_x} = \alpha_x \mu q \quad (1)$$

where $q = dv/d\theta$. The differential dw_x can be eliminated by use of expression

$$dw_x = \rho_s (1 - \epsilon)\, dx \quad (2)$$

Substituting for dw_x in (1) one gets

$$g_c \frac{dp_s}{dx} = \mu \rho_s (1 - \epsilon)\, \alpha_x q \quad (3)$$

Under certain conditions (*11*) q may vary markedly throughout the solid and may not be treated as a constant. For relatively dilute slurries and long filtration cycles however q may be considered as approximately constant. Solving for dx in (3) and placing limits on the integrals one obtains

$$\int_0^x dx = x = \frac{g_c}{\mu \rho_s q} \int_0^{p_s} \frac{dp_s}{\alpha_x (1 - \epsilon)} \quad (4)$$

where the upper limit of the integral p_s is related to the hydraulic pressure by

$$p_s = p - p_1 \quad (5)$$

The quantity p_1 represents the pressure required to overcome the resistance of the medium and will be neglected in this paper. If the integration is carried out over the entire cake, the limits on distance and compressive pressures at the interface of the cake and medium will be given by $x = L$, the thickness of the cake, and $p_s = p$, the applied pressure at the surface of the cake. Equation (4) becomes on integration from 0 to L

Harrison Cooper is at the University of Southern California, Los Angeles, California.

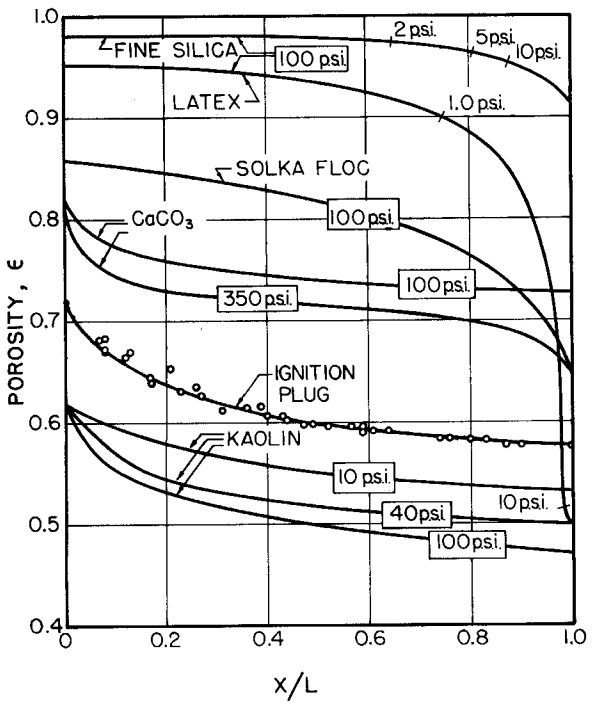

Fig. 1. Calculated values of ϵ vs. x/L.

$$L = \frac{g_c}{\mu \rho_s q} \int_0^p \frac{dp_s}{\alpha_x (1 - \epsilon)} \quad (6)$$

Dividing Equation (4) by (6) one gets

$$\frac{x}{L} = \frac{\int_0^{p_s} \frac{dp_s}{\alpha_x (1-\epsilon)}}{\int_0^p \frac{dp_s}{\alpha_x (1-\epsilon)}} = f(p_s) \quad (7)$$

In Equation (7) the integral in the denominator is constant at any given total pressure p. The integral in the numerator is a function of the upper limit of integration, and consequently Equation (7) defines a relationship between x/L and p_s. As ϵ is a function of p_s as obtained from a consolidometer or from compression-permeability cell measurements, Equation (7) may be used to relate x/L to ϵ. Shirato and Okamura (8) developed similar expressions for calculating the porosity variation aand obtained valuable experimental data.

Figure 1 shows curves of calculated values for porosity vs. fractional distance measured from the cake surface for a number of substances for which the porosity and specific resistance values of Grace (2) were employed. For comparison experimental data of Shirato and Okamura (8) for ignition plug are included.

As the filtration pressure is increased, the surface porosity at $x/L = 0$ remains constant, as indicated for kaolin and calcium carbonate. As the pressure increases, the porosity curves seek lower levels.

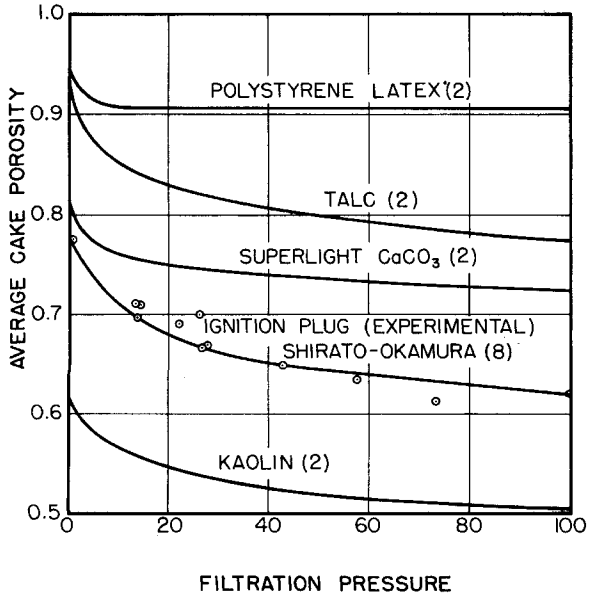

Fig. 2. Calculated values of average cake porosity vs. applied filtration pressure.

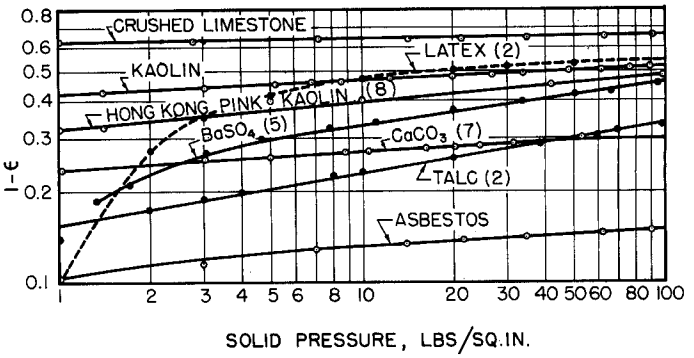

Fig. 3. Logarithmic plot of $1-\epsilon$ vs. solid pressure.

The porosity variations for two highly compressive materials, silica and polystyrene latex, demonstrate relatively slight calculated changes of porosity with distance through the filter bed, as illustrated in Figure 1. The drop in volume percentage of liquid from 98 to 91% in the fine silica cake does not at first appear to be particularly large. The increase in solid content from 2 to 9% corresponds to a large shrinkage in the cake. If 100 lb. of fine silica cake with 2% solids by volume (0.85% by weight) containing 99.15 lb. of water is increased to 9% solids by volume, approximately 90 lb. of water will be removed. Small porosity changes of highly porous materials may cause large volume changes in cakes.

The solid pressure ($p_s = p - p_x$) at several depths is indicated on the curves for fine silica and polystyrene latex. For the latter substance the solid pressure, which is zero at the surface ($x/L = 0$), requires 75% of the thickness of the solid to increase to 1.0 lb./sq. in. Correspondingly the hydraulic pressure drops 1 lb./sq. in. from 100 to 99 lb./sq. in. in the same fractional distance. The value of p_s does not reach 10 lb./sq. in. until $x/L = 0.98$; consequently 90% of the pressure drop of the flowing fluid occurs in the last 2% of the solid thickness. A similar, although less extreme, situation occurs with fine silica, where 90% of the hydraulic pres-

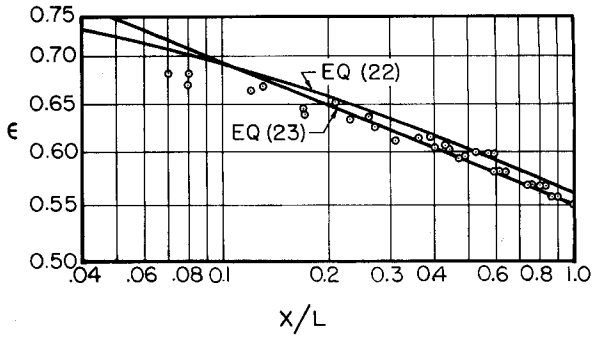

Fig. 4. Calculated and experimental values of ϵ vs. x/L Hong Kong pink kaolin.

sure drop is concentrated in the last 12% of the solid.

AVERAGE POROSITY

In process calculations the average liquid content is of more interest than the curves of porosity variation with distance. The average porosity may be obtained by graphical integration of the curves in Figure 1 in accordance with the equation

$$\epsilon_{avg} = \frac{1}{L}\int_0^L \epsilon\, dx \qquad (8)$$

The average porosity may also be calculated with the use of the following equation, previously presented by the author (*11*) and also developed by Shirato and Okamura (*8*):

$$\epsilon_{avg} = 1 - \frac{\int_0^p \frac{dp_s}{\alpha_x}}{\int_0^p \frac{dp_s}{\alpha_x(1-\epsilon)}} \qquad (9)$$

The frequently used ratio m of mass of wet cake to mass of dry solid in the cake is given by

$$m = 1 + \frac{\rho\,\epsilon_{avg}}{\rho_s(1-\epsilon_{avg})} \qquad (10)$$

In Figure 2 the calculated average porosity vs. total pressure is illustrated for a number of materials and includes comparison with the experimental data of Shirato and Okamura (*8*) for an ignition plug slurry. In the case of polystyrene latex little advantage would accrue to increases in pressure insofar as reduction in liquid content is concerned. Although polystyrene latex is highly compressible, there is little compaction of the cake until the medium is approached as indicated in Figure 1. Because of the small hydraulic pressure drop through a major portion of the cake the average porosity remains high.

Analytical Formulas for Average Porosity

The curves of Figure 2 indicate that a priori prediction of the effect of pressure on liquid content is difficult and not entirely dependent on the compressibility of the solid. An analytical expression relating ϵ_{avg} to p is desirable as it will assist in determining the relative effects of p in the integrals shown in Equation (9). Previously (9) it has been shown that for moderately compressible materials it is possible to represent both porosity and local specific resistance by power functions of the compressive pressure as follows:

$$\alpha_x = \alpha_o p_s^n \quad p_s > p_i \qquad (11)$$

$$\alpha_x = \alpha_i = \alpha_o p_i^n \quad p_s < p_i \qquad (12)$$

$$\epsilon = \epsilon_o p_s^{-\lambda} \quad p_s > p_i \qquad (13)$$

$$\epsilon = \epsilon_i = \epsilon_o p_i^{-\lambda} \quad p_s < p_i \qquad (14)$$

where p_i is a low pressure in the range of 0.1 to 1.0 lb./sq. in. The approximations represented by (11) and (13) result from the linearity of logarithmic plots of α_x and ϵ vs. p_s in the region up to 100 lb./sq. in. and for values of n less than roughly 0.5 to 0.7. As p_s approaches zero, Equations (11) and (13) must be abandoned, as they yield an infinite value for ϵ and zero for α_x. Experimentally both α_x and ϵ approach limiting values which are defined as α_i and ϵ_i. For pressures ranging from zero to p_i it is satisfactory in the mathematical formulation to assume that α_x and ϵ are constant. Virtually no data are available for pressures below 1.0 lb./sq. in. Analysis of the systems in Table 1 indicates that the power function can be used as low as the given values of p_i.

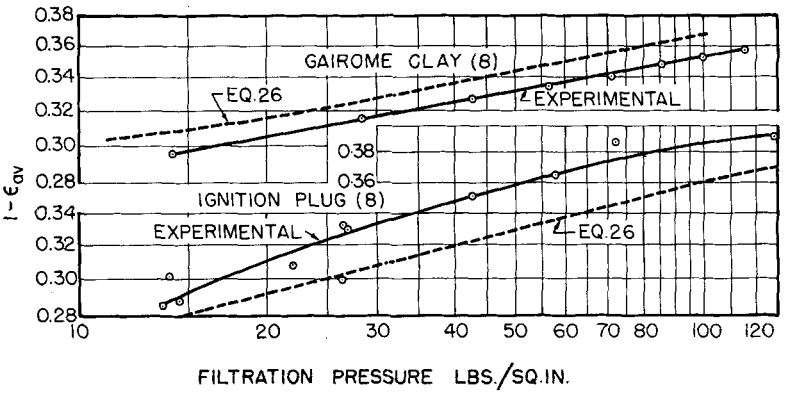

Fig. 6. Comparison of experimental and calculated values of average porosity vs. applied filtration pressure for ignition plug and gairome clay.

In Equation (9) the quantity $(1-\epsilon)$ occurs as a part of the integral appearing in the denominator. Simplification of resulting analytical formulas can be effected by representing $(1-\epsilon)$ as a power function of p_s. In Figure 3 a logarithmic plot of $(1-\epsilon)$ vs. p_s illustrates a general linear relation which exists. For the highly compressible polystyrene latex, represented by a dotted line, the approximate power function cannot be used. For moderately compressible materials like kaolin and talc the data may be interrelated by

$$1-\epsilon = Bp_s^{\beta} \quad p_s > p_i \qquad (15)$$

While it may seem peculiar to represent both ϵ and $(1-\epsilon)$ by different power functions, the relatively limited changes in porosity permit the data to be accurately rectified by Equations (13) and (15). Below pressure p_i the porosity is assumed constant, and Equation (15) reduces to

$$1-\epsilon_i = Bp_i^{\beta} \quad p_s < p_i \qquad (16)$$

Values of B and β for several substances are given in Table 2.

In order to relate ϵ to x/L the two integrals of Equation (7) must be evaluated. Beginning with the integral in the numerator, which will be called I, one can substitute for α_x and $1-\epsilon$ in the following manner:

$$I = \int_0^{p_s} \frac{dp_s}{\alpha_x(1-\epsilon)} = \int_0^{p_i} \frac{dp_s}{\alpha_i(1-\epsilon_i)} + \int_{p_i}^{p_s} \frac{dp_s}{\alpha_o B\, p_s^{n+\beta}} \qquad (17)$$

where α_i and ϵ_i are considered constants. Integrating and substituting limits one gets

$$I = \frac{p_i}{\alpha_i(1-\epsilon_i)} + \frac{1}{\alpha_o B}\,\frac{p_s^{1-n-\beta} - p_i^{1-n-\beta}}{n+\beta-1} \qquad (18)$$

Substituting for α_i from (12) and $(1-\epsilon_i)$ from (16) and rearranging Equation (18) one obtains

$$I = \frac{1}{\alpha_o B}\,\frac{p_s^{1-n-\beta} - (n+\beta)\,p_i^{1-n-\beta}}{1-n-\beta} \qquad p > p_i \qquad (19)$$

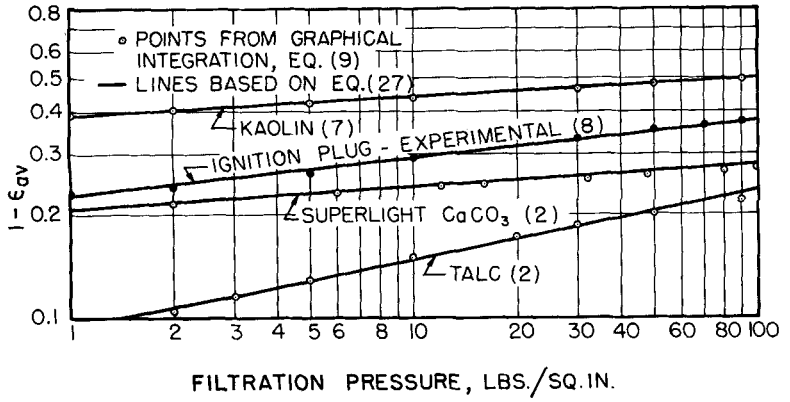

Fig. 5. Comparison of numerical integration for average porosity with Equation (9).

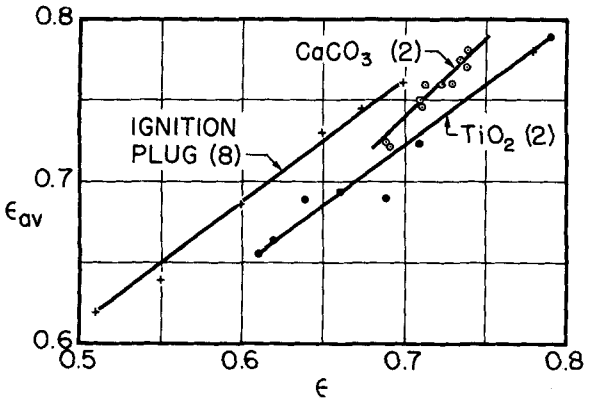

Fig. 7. Average vs. local porosity at same pressure.

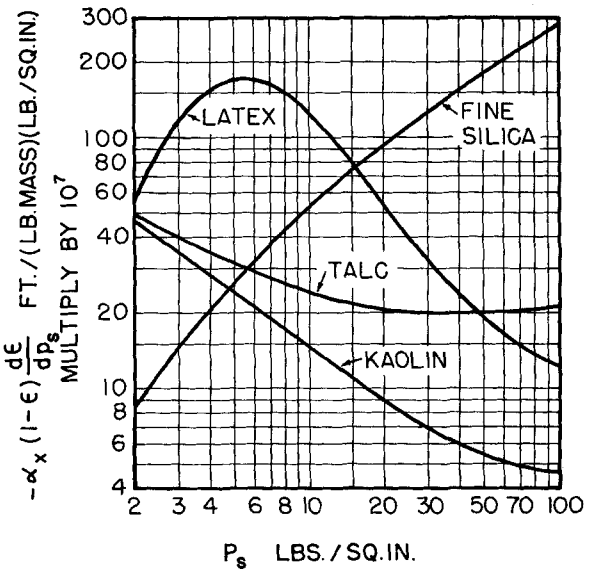

Fig. 8. Graph for determining slope of local porosity vs. x/L in filter cakes.

The integral of the denominator of Equation (7) has the same form as (19) except that the total pressure p replaces p_s. Substitution of the analytical expressions for the integrals in (7) produces

$$\frac{x}{L} = \frac{p_s^{1-n-\beta} - (n+\beta)\, p_i^{1-n-\beta}}{p^{1-n-\beta} - (n+\beta)\, p_i^{1-n-\beta}} = \frac{p_s^{1-n-\beta} - \text{const}}{p^{1-n-\beta} - \text{const}} \quad (20)$$

If p is large compared with p_i and n is less than approximately 0.5 to 0.7, the constant term in the numerator and denominator can be eliminated to give

$$\frac{x}{L} = \left(\frac{p_s}{p}\right)^{1-n-\beta} = \left(1 - \frac{p_x}{p}\right)^{1-n-\beta} \quad (21)$$

Elimination of p_s in favor of ϵ in Equations (20) and (21) leads to

$$\frac{x}{L} = \frac{\epsilon_0^{1/\lambda}\, \epsilon^{-(1-n-\beta)/\lambda} - (n+\beta)\, p_i^{1-n-\beta}}{p^{1-n-\beta} - (n+\beta)\, p_i^{1-n-\beta}} \quad (22)$$

or for the more simple form in which p_i is neglected

$$\frac{x}{L} = \left(\frac{\epsilon}{\epsilon_1}\right)^{-(1-n-\beta)/\lambda} \quad (23)$$

where ϵ_1 is the porosity at the maximum pressure p.

Figure 4 compares Equations (22) and (23) as applied to the data of Shirato and Okamura (8) for Hong Kong pink kaolin. Values used in making the comparisons are as follows: p = 42.2 lb./sq. in., ϵ_1 = 0.55 (experimental), ϵ_0 = 0.695 (calculated), n = 0.332 [calculated by Shirato and Okamura (8)], λ = 0.0586 (calculated by Tiller and Cooper), β = 0.095 (calculated by Tiller and Cooper), and p_i = 0.5 lb./sq. in. Equations (22) and (23) are about equally good for representing the data through most of the filter solid. As the cake surface is approached however Equation (22) gives better results, as would be expected since the p_i term was not neglected.

To obtain an analytical expression for the average porosity as a function of total pressure either Equation (8) or Equation (9) can be used as a basis for integration of the empirical relations. As the integral in the denominator in Equation (9) has already been found, it is necessary to calculate the integral in the numerator as follows:

$$\int_0^p \frac{dp_s}{\alpha_x} = \int_0^{p_i} \frac{dp_s}{\alpha_i} + \int_{p_i}^p \frac{dp_s}{\alpha_0 p_s^n} \quad (24)$$

Integrating and simplifying one gets

$$\int_0^p \frac{dp_s}{\alpha_x} = \frac{1}{\alpha_0} \frac{p^{1-n} - n p_i^{(1-n)}}{1-n} \quad (25)$$

Substituting in Equation (8) for the two integrals one obtains

$$\epsilon_{avg} = 1 - B\left(\frac{1-n-\beta}{1-n}\right) \frac{p^{1-n} - n\, p_i^{1-n}}{p^{1-n-\beta} - (n+\beta)\, p_i^{1-n-\beta}} \quad (26)$$

Neglecting p_i and rearranging one gets

$$1 - \epsilon_{avg} = B\left(\frac{1-n-\beta}{1-n}\right) p^{\beta} \quad (27)$$

Figure 5 compares the formula of Equation (27) with the values obtained by the numerical integration of Equation (9), the agreement being quite good.

Figure 6, compares experimental data for ignition plug and Gairome clay (8) with calculations based upon Equation (26). The agreement is good, although the differences are magnified by the large scale for the log $(1 - \epsilon_{avg})$ Equation (27) gives somewhat less satisfactory values. Both Equations (26) and (27) yield slopes which are quite close to those of the experimental values. The constant B can be adjusted so that the calculated curve nearly coincides with the experimental data. Values used in performing calculations for Figure 6 are as follows:

	Gairome clay	Ignition plug
Sp. gr.	2.62	3.23
ϵ_0	0.815	0.745
ϵ_i	0.800	0.78
n*	0.60*	0.56*
λ	0.091	0.07
β	0.129	0.128
B	0.26	0.27
p_i lb./sq. in.	1.3	0.6

* Values calculated by Okamura and Shirato (8).

TABLE 1

Substance	ϵ_i	p_i, lb./sq. in.	ϵ_0*	λ	Literature cited
Crushed limestone	0.375	1.0	0.375	0.015	(9)
Hyflo	0.872	0.9	0.88	0.014	(9)
Asbestos	0.902	0.9	0.90	0.017	(9)
Kaolin	0.698	0.03	0.59	0.045	(9)
Kaolin, Hong Kong pink	0.72	0.6	0.70	0.059	(8)
Ignition plug	0.78	0.6	0.75	0.07	(8)
Calcium carbonate	0.771	0.9	0.77	0.034	(7)

* These values of ϵ_0 imply that p_s is expressed in pounds per square inch.

Approximation for Average Porosity

Returning to Equation (26), one can rearrange the terms so that

$$1 - \epsilon_{avg} = Bp^{\beta}\left(\frac{1-n-\beta}{1-n}\right)\left[1 + \frac{\beta}{(p/p_i)^{1-n} - (n+\beta)\,(p/p_i)^{\beta}}\right] \quad (28)$$

TABLE 2

Substance	B	β	Literature cited
Gairome clay	0.26	0.13	(8)
Ignition plug	0.27	0.13	(8)
Calcium carbonate	0.235	0.063	(2)
Kaolin	0.42	0.054	(8)
Talc	0.155	0.203	(2)
Asbestos	0.115	0.057	(9)

The quantity $B_p^{\beta} = 1 - \epsilon$. With $z = p/p_i$

$$1 - \epsilon_{avg} = \left(\frac{1 - n - \beta}{1 - n}\right)(1 - \epsilon)\left[1 + \frac{\beta}{z^{1-n} - (n + \beta)\, z^{\beta}}\right] \quad (29)$$

As the pressure increases, in many cases the factor containing p_i can be neglected and Equation (29) reduces to

$$1 - \epsilon_{avg} = \text{constant}\ (1 - \epsilon) \quad (30)$$

where ϵ_{avg} and ϵ are compared at equal pressures. In accordance with Equation (30) ϵ_{avg} will plot approximately as a linear function of ϵ, or $(1 - \epsilon_{avg})$ will be linear in $(1 - \epsilon)$. Logarithmic plots of $(1 - \epsilon_{avg})$ and $(1 - \epsilon)$ vs. pressure will be parallel and separated by the logarithm of the constant in Equation (30). It should be noted that ϵ is the local porosity at a given pressure and ϵ_{avg} is the average porosity of a cake at the same pressure.

In Figure 7 plots of ϵ_{avg} vs. • are shown for superlight calcium carbonate, R110 titanium dioxide, and ignition plug. The linearity of the plots is within the accuracy of the data. In general the less compressible the material the more nearly the slope will approach unity.

For practical purposes Equation (27) can be improved if the multiplier of the pressure term is replaced by an experimentally determined value in the form

$$1 - \epsilon_{avg} = (1 - \epsilon_{avg_o})\left(\frac{p}{p_o}\right)^{\beta} \quad (31)$$

where ϵ_{avg_o} is the average porosity (determined from an experimental value of m) at pressure p_o. The value of ϵ_{avg_o} could be conveniently found from a constant pressure filtration or from a variable-pressure filtration in which p_o was the maximum pressure. The exponent β may be derived from consolidometer-determined porosities as a function of loading pressures.

Slope of the Porosity Curve

It was previously pointed out that Hutto (4) expressed the opinion that the slopes of porosity vs. distance curves of various investigators were incompatible. All Hutto's experimental curves showed a large slope (negative) at the cake surface with decreasing rates of change of ϵ with x as the supporting medium was approached. Essentially the second derivative $d^2\epsilon/dx^2$ in Hutto's experiments was positive, and he considered negative values impossible. Analysis of the compression-permeability cell data of Grace (2) indicates that both types of variation are possible. In addition it was found that a change from one type to the other was possible and that the second derivative could be both positive and negative for the same substance.

The slope of the ϵ vs. x curve can be written in the form

$$\frac{d\epsilon}{dx} = \frac{d\epsilon}{dp_s}\frac{dp_s}{dx} \quad (32)$$

The derivative dp_s/dx can be replaced by the use of Equation (3); thus

$$\frac{d\epsilon}{dx} = \frac{\mu \rho_s q}{g_c}(1 - \epsilon)\frac{d\epsilon}{dp_s}\alpha_x \quad (33)$$

Since $d\epsilon/dp_s$ is always negative, $d\epsilon/dx$ will be negative. The second derivative of Equation (33) determines the behavior of the slope of the ϵ vs. x curve. Figure 8 shows a logarithmic plot of $-\alpha_x(1 - \epsilon)\, dp_s/dx$ as a function of p_s. The second derivative is given by

$$\frac{g_c}{\mu \rho_s q}\frac{d^2\epsilon}{dx^2} = \frac{d}{dp_s}\left[\alpha_x(1 - \epsilon)\frac{d\epsilon}{dp_s}\right]\frac{dp_s}{dx} \quad (34)$$

Thus the slope (converted to rectangular coordinates) of the curves in Figure 8 multiplied by dp_s/dx will give the second derivation. Since four completely different trends are clearly indicated for the four substances, Hutto was in error. The greatest rate of change of porosity may occur either at the surface (kaolin) or at the medium (fine silica). The porosity curves may pass through points of inflection, as is the case with talc and latex.

SUMMARY

It is shown that a plot of ϵ_x vs. x can take on a variety of shapes for different materials subject only to the condition that ϵ_x decreases as the fluid flows from the surface through the cake to the medium.

NOTATION

B = constant defined by Equation (15)
g_c = conversion factor, poundals/lb.-force or (lb.-mass) (ft.)/(lb.-force) (sec.^{2})
L = cake thickness, ft.
m = ratio of mass of wet to mass of dry cake
n = compressibility coefficient defined by Equation (11)
p = applied filtration pressure, lb.-force/sq. ft.
p_i = low pressure below which porosity is constant, lb.-force/sq. ft.
p_s = solid compressive pressure $p - p_x$, lb.-force/sq. ft.
p_x = liquid pressure at x ft. from surface, lb.-force/sq. ft.
p_i = pressure at interface of supporting medium and cake, lb.-force/sq. ft.
p_o = pressure at which ϵ_{avg} is known, lb.-force/sq. ft.
q = rate of filtration, cu. ft./(sq. ft.) (sec.)
x = distance from surface of filter cake, ft.
w_x = mass of dry filter cake per unit area deposited in first x ft., lb.-mass/sq. ft.
z = ratio of p/p_i

Greek Letters

α = average specific filtration resistance, ft./lb.-mass
α_x = local specific filtration resistance, ft./lb.-mass
α_i = value of α when $p < p_i$, ft./lb.-mass
α_o = constant defined in Equation (11)
β = exponent defined in Equation (15)
ϵ = local porosity
ϵ_{avg} = average porosity
ϵ_o = constant defined by Equation (13)
ϵ_{avg_o} = average porosity at pressure p_o
ϵ_i = local porosity at pressure p
λ = exponent defined by Equation (13)
μ = viscosity, lb.-mass/(ft.) (sec.)
ρ = liquid density, lb.-mass/cu. ft.
ρ_s = true solid density, lb.-mass/cu. ft.

LITERATURE CITED

1. Cooper, Harrison, M.S. thesis, Univ. Houston, Houston, Texas (1958).
2. Grace, H. P., *Chem. Eng. Progr.*, **49**, 303, 367 (1953).
3. ———, *Chem. Eng. Progr. Symposium Ser. No. 25*, **55**, 151 (1959).
4. Hutto, F. B., Jr., *Chem. Eng. Progr.*, **53**, 328 (1957).
5. Kottwitz, Frank, Ph.D. thesis, Iowa State Univ., Ames, Iowa (1955).
6. Rietema, K., *Chem. Eng. Sci.*, **2**, 88 (1953).
7. Ruth, B. F., *Ind. Eng. Chem.*, **38**, 564 (1946).
8. Shirato, M., and S. Okamura, *Chem. Eng. (Japan)*, **19**, 104, 111 (1955); **20**, 98, 678 (1956); **23**, 11, 226 (1959).
9. Tiller, F. M., *Chem. Eng. Progr.*, **49**, 467 (1953); **51**, 282 (1955).
10. ———, *A.I.Ch.E. Journal*, **4**, 170 (1958).
11. ———, and Harrison Cooper, *ibid.*, **6**, 595 (1960).
12. Young, G. J., *Trans. Am. Inst. Min. Eng.*, **42**, 752 (1911).

Manuscript received February 10, 1960; revision received January 8, 1962; paper accepted January 10, 1962. Paper presented at A.I.Ch.E. Atlanta meeting.